

# Mapping of *Phragmites* in estuarine wetlands using high-resolution aerial imagery

Matthew Walter · Pinki Mondal

Received: 7 December 2022 / Accepted: 28 February 2023 / Published online: 17 March 2023 © The Author(s), under exclusive licence to Springer Nature Switzerland AG 2023

**Abstract** *Phragmites australis* is a widespread invasive plant species in the USA that greatly impacts estuarine wetlands by creating dense patches and outcompeting other plants. The invasion of *Phragmites* into wetland ecosystems is known to decrease biodiversity, destroy the habitat of threatened and endangered bird species, and alter biogeochemistry. While the impact of *Phragmites* is known, the spatial extent of this species is challenging to document due to its fragmented occurrence. Using high-resolution imagery from the National Agriculture Imagery Program (NAIP) from 2017, we evaluated a geospatial method of mapping the spatial extent of *Phragmites* across the state of DE. Normalized difference vegetation index (NDVI) and principal component analysis (PCA) bands are generated from the NAIP data and used as inputs in a random forest classifier to achieve a high overall accuracy for the Phragmites classification of around 95%. The classified gridded dataset has a spatial resolution of 1 m and documents the spatial distribution of Phragmites throughout the state's estuarine wetlands (around 11%). Such detailed classification could aid in monitoring the spread of this invasive species over space and time and would inform the decision-making process for landscape managers.

**Keywords** *Phragmites* · Machine learning · Classification · Invasive · Vegetation

#### Introduction

Invasive species are living organisms that spread rapidly within an environment, typically outcompeting other organisms, leading to changes in ecosystem processes and functioning (Ehrenfeld, 2010; Linders et al., 2019; Vitousek et al., 1996). The cost of ecosystem loss and required management associated with invasive species was estimated to potentially reach \$162.7 billion worldwide in 2017, a threefold increase per decade since 1970 (Diagne et al., 2021). The spread of non-native plant species through the global horticulture trade and increasing global temperatures have created the conditions for increased occurrences of biological invasions (Bertelsmeier et al., 2013; Bradley et al., 2012; Hellmann et al., 2008; Reichard & White, 2001). Phragmites australis, also known as common reed, has become a dominant plant in the wetlands of North America (Chambers et al., 1999). There are two subspecies of Phragmites australis in North America, one native (subsp. americanus) and one non-native (subsp. australis) (Saltonstall, 2002, 2003; Saltonstall et al., 2004). Non-native *Phragmites* is considered invasive in North America because of its rapid expansion, especially in tidal areas, and the ability to outcompete other marsh plants, while native *Phragmites* is non-invasive and much less common (Marks et al., 1994; Saltonstall,

M. Walter (☑) · P. Mondal Department of Geography and Spatial Sciences, University of Delaware, Newark, DE 19716, USA e-mail: mswalter@udel.edu

P. Mondal

e-mail: mondalp@udel.edu

P. Mondal
Department of Plant and Soil Sciences, University
of Delaware, Newark, DE 19716, USA
e-mail: mondalp@udel.edu



2002). In this paper, we use "*Phragmites*" in reference to the non-native subspecies.

Phragmites is commonly found in wetland areas; however, it also grows in dry upland areas (Avers et al., 2014). It is a perennial grass that grows taller than most marsh plants at 2 to 5 m in height, growing in large dense patches (Saltonstall et al., 2004). Habitat alterations caused by the invasion of Phragmites include the reduction of marsh edge, increased aboveground biomass, and decreased salinity levels (Windham & Lathrop, 1999). Moreover, Phragmites lowers plant biodiversity by outcompeting marsh plant species and communities such as Typha spp., marsh meadow, and sedge/grass hummock (Wilcox et al., 2003). These alterations and losses in plant biodiversity negatively affect many critical animal species living in marsh habitats. Wetlands dominated by *Phragmites* patches were shown to have significantly fewer bird species and decreased success of turtle nesting (Benoit & Askins, 1999; Bolton & Brooks, 2010; Robichaud & Rooney, 2017).

Human disturbances to wetland ecosystems have been found to increase the spread of *Phragmites*. For example, the conversion of wetlands to other land uses such as ditches and roads facilitates the spread of *Phrag*mites by creating conditions in which *Phragmites* can survive, including high variations in water level and exposure to deicing salt (Jodoin et al., 2008). A strong link has also been made between shoreline development and the invasion of *Phragmites*, with over 90% of intermarsh variation of *Phragmites* cover attributed to shoreline development in New England salt marshes (Silliman & Bertness, 2004). Other disturbances such as increased nutrient loads and clearing of other vegetation also facilitate the spread of *Phragmites* (Kettenring et al., 2012; Minchinton & Bertness, 2003). Phragmites invasions are of particular concern in coastal regions where marsh migration is occurring due to sea level rise (Schieder et al., 2018). Sea level rise is a major driver of saltwater intrusion, the encroachment of saline water into inland coastal ecosystems, facilitating marsh migration (Gedan & Fernández-Pascual, 2019). Saltwater intrusion creates an opportunity for the salt-tolerant *Phragmites* to invade where other plants have been displaced (Tully et al., 2019). In the Delaware Bay, 32% of the forest area lost due to saltwater intrusion was populated by a *Phragmites*dominated salt marsh in 2006 (Smith, 2013).

To combat the negative effects caused by *Phragmites*, many local governments have developed Phragmites control programs. For example, the Delaware Phragmites Control Cost-Share Program offered by the Delaware Division of Fish and Wildlife and the U.S. Department of Agriculture's Natural Resources Conservation Program (USDA NRCS) provides technical and financial assistance to landowners with wetlands invaded by Phragmites on their properties (DNREC, 2022). In the USA, land managers from public and private conservation organizations spent more than \$4.6 million per year on Phragmites management between 2005 and 2009 (Martin & Blossey, 2013). Methods of *Phragmites* control rely on repeated cutting, burning, and application of herbicide (Hazelton et al., 2014; Mal & Narine, 2004). For *Phragmites* control efforts to be successful, it is critical to have accurate information on the geographic location and extent of invasions (Anderson et al., 2021; Bourgeau-Chavez et al., 2013). Thus, large-scale maps of *Phragmites* are a critical tool in *Phragmites* control. Remote sensing imagery can be utilized to create accurate maps of *Phragmites* while reducing the time and labor costs of in situ methods of detection. Furthermore, Phragmites management may benefit from watershedscale control efforts in coastal regions (Hazelton et al., 2014). Remote sensing techniques enable mapping at large spatial scales and thus have the potential to increase the effectiveness of *Phragmites* control efforts.

The effectiveness of remote sensing classifications for the mapping of *Phragmites* to inform control efforts is reliant on the spatial resolution, geographic extent, temporal resolution, and availability of the remotely sensed imagery. To control *Phragmites*, the location of invasions should be known with accuracy and precision. Previous research has mapped *Phragmites* with moderateresolution datasets and achieved user's accuracy from 43 to 91% for Phragmites (Bourgeau-Chavez et al., 2013, 2015; Rupasinghe & Chow-Fraser, 2019). Data should also be available at large spatial and temporal scales for effective and repeated watershed-level control efforts. Many studies have mapped *Phragmites* at a high resolution through the use of unmanned aerial systems (UAS) with user's accuracy for *Phragmites* ranging from 31 to 82% (Abeysinghe et al., 2019; Anderson et al., 2021). One disadvantage of relying on UAS for Phragmites mapping is that the data collected through these efforts are not readily available throughout the USA and often



cover a small spatial extent. To address these challenges, we utilized high-resolution (1 m) aerial imagery from the National Agriculture Imagery Program (NAIP) to map Phragmites with higher accuracy and precision compared to datasets reliant on moderate-resolution imagery. NAIP data is collected at the state scale for every state in the USA on an approximately 2- to 3-year cycle with data going back to 2003. The state-level geographic scale of NAIP data also enables its use for statewide analysis. Additionally, NAIP data is freely available and accessible through Google Earth Engine (GEE), making it easily accessible for efforts of *Phragmites* control. Previous research has used NAIP images to manually identify Phragmites to create a dataset to train a machine-learning model with moderate-resolution Landsat images as input (Liu et al., 2016a). Other studies have also mapped Phragmites by using NAIP imagery as an input into machine learning classifiers (Correll et al., 2019; Liu et al., 2016b; Xie et al., 2015). While NAIP imagery has been successfully used for Phragmites classification, reviews of image classification based on NAIP imagery alone indicate that the spectral limitations of NAIP can lead to decreases in accuracy (Maxwell et al., 2017). To address this limitation, Maxwell et al. (2017) suggested simplifying NAIP-based classifications by aggregating classes together and using spectral ratios to increase classification accuracy.

Here, we built upon previous methods of NAIP-based classifications of *Phragmites* and addressed the limitations of NAIP by focusing on only three land cover classes and using a normalized difference vegetation index (NDVI) in our analysis. Furthermore, we evaluated the use of principal component analysis (PCA) to create additional input bands to improve the accuracy of our classification. This new method of classifying *Phragmites* with combined NAIP bands, NAIP-derived NDVI, and PCA bands was used to quantify the spatial distribution of *Phragmites* across the State of DE. In this paper, we answer the following questions:

- 1. Can high-resolution NAIP imagery be used to accurately classify *Phragmites* in the state of DE?
- 2. Does the use of NDVI and PCA along with NAIP spectral bands lead to higher accuracy in the mapping of *Phragmites* when compared to using just NAIP bands?
- 3. What is the spatial extent of *Phragmites* in DE in 2017?

#### Materials and methods

Study area

The eastern USA state of Delaware (DE) borders the Atlantic Ocean and is comprised of three counties from north to south, New Castle, Kent, and Sussex (Fig. 1). With an average elevation of just 18 m above sea level, DE has a high number of tidal and non-tidal wetlands in which Phragmites grows. Other types of vegetation commonly found in DE's estuarine wetlands include narrowleaf cattail (Typha angustifolia), marsh elder (Iva frutescens), saltmarsh cordgrass (Spartina alterniflora), big saltmarsh cordgrass (Spartina cynosuroides), seaside goldenrod (Solidago sempervirens), three-square bulrush (Schoenoplectus pungens), and spike saltgrass (Distichlis spicata) (NWI, 1985). Although Phragmites is also found in freshwater wetlands, we have mapped them in estuarine wetlands within DE (Fig. 1) which comprise the majority of DE's non-forested wetlands, where *Phragmites* is the most prevalent (NWI, 1985; Saltonstall, 2002). We used the wetlands map produced by Delaware Department of Natural Resources and Environmental Control (DNREC) and the Conservation

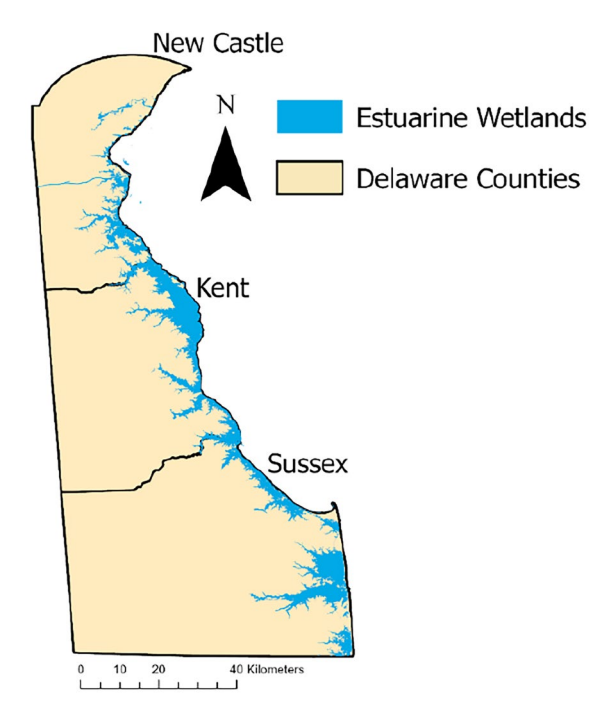


Fig. 1 The distribution of estuarine wetlands within DE



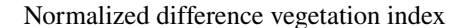
Management Institute (CMI) at Virginia Polytechnic Institute and State University (Virginia Tech) for the National Wetlands Inventory (NWI) to delineate only estuarine wetlands—the study area here (U.S. Fish & Wildlife Service, 2018). The total area of the estuarine wetlands in DE is around 460 km<sup>2</sup>.

### Aerial imagery data

To identify *Phragmites*, freely available high-resolution imagery was used from NAIP, which is run by the United States Department of Agriculture (USDA) and acquires high-resolution (1 m) aerial imagery of Earth's surface over the continental USA (NAIP, 2012). The imagery provides spectral information in the red, green, and blue channels beginning in 2003. Spectral information in the near-infrared (NIR) channel also became available starting in 2007 for some states (NAIP, 2012). NAIP data was originally collected once on a 5-year cycle, but switched to a general 3-year cycle beginning in 2009 (NAIP, 2012).

NAIP imagery is commonly used for land monitoring purposes, such as mapping forest characteristics at a high-resolution (Basu et al., 2015; Davies et al., 2010; Hogland et al., 2018), or increasing classification accuracy for mapping complex urban areas (Hayes et al., 2014; Nagel & Yuan, 2016). We used NAIP data for classifying Phragmites due to its high-resolution and demonstrated application in plant classification (Correll et al., 2019; Liu et al., 2016b; Xie et al., 2015). However, NAIP data have some drawbacks such as inconsistent temporal coverage within a year, low radiometric resolution (8-bit) when compared to satellite sensors, and large shadows in proximity to trees, buildings, and other large structures. NAIP data is typically captured at the height of the growing season when *Phragmites* is at its peak growth stage. Due to the lack of trees and buildings in most estuarine wetland areas, shadows also had little effect on our classification.

The cloud-based geospatial data processing platform GEE was used for data compilation, processing, and classification. GEE allows easily reproducible analyses through its freely available script-based interface and efficient processing of large datasets (Gorelick et al., 2017). For this study, we used all four spectral bands (red, green, blue, and NIR) from the most recently captured NAIP imagery in July 2017. Available NAIP scenes in DE were mosaiced and clipped to the boundary of all estuarine wetlands throughout the state.



To assess the use of spectral indices in our classification, we calculated NDVI from the NAIP imagery. NDVI is a proxy for vegetation health based on the greenness of a vegetation "pixel" using bands from the NIR and red portions of the electromagnetic spectrum. NDVI is calculated using the following equation (Rouse et al., 1974; Townshend et al., 1985; Tucker et al., 1985):

$$NDVI = \frac{NIR - red}{NIR + red}$$

NAIP-derived NDVI has previously been used as an input band for land cover classifications because of the additional information it provides in distinguishing different vegetation types. (Hayes et al., 2014; Li et al., 2014).

For NAIP data to be effectively used for differentiating Phragmites from other marsh plants, Phragmites should have a distinct spectral signature during the summer months of June and July when NAIP images are usually captured. To ensure the suitability of NAIP summer images for classifying *Phragmites*, the vegetation phenology of DE's estuarine wetlands was assessed using Sentinel-2 images. A time series of monthly NDVI values for the entire year of 2017 was plotted for each of the three land cover classes using 10-m Sentinel-2 Level-1C images. Level-1C top of atmosphere reflectance was used over Level-2A bottom of atmosphere reflectance because Level-2A imagery was not globally generated until December 2018. Sentinel-2 has been frequently used in phenology research due to its high revisit frequency of 5 days and higher spatial resolution (10 m) than other publicly accessible satellites such as Landsat (30 m) (Misra et al., 2020). NDVI was used as an indicator to track phenological differences in Phragmites and other vegetation because of its ability to estimate plant growth (Wu et al., 2017). Monthly medians were calculated for each of the 12 months in 2017 when the NAIP data was collected. Sentinel-2 images were cloud masked using the QA60 band in GEE.

#### Principal component analysis

We also assessed the use of additional band transformations through PCA. PCA is a data reduction method that converts potentially correlated variables into a set of



uncorrelated variables (Jolliffe & Cadima, 2016; Pearson, 1901). In our study, five PCA bands were derived from four spectral bands and one NDVI band. The PCA bands were calculated in GEE using the eigenanalysis workflow available on the platform (GEE, 2022). First, the input images were converted to 1-D arrays, from which a variance-covariance matrix was calculated. Next, the "eigen" command was used to calculate eigenvalues and eigenvectors for the variance-covariance matrix. The original image array was then multiplied by the eigenvectors to calculate the principal components. Finally, the principal components were normalized by their standard deviations. PCA has been used in remote sensing image classification both for reducing data dimensions and directly as input bands to be used in classifying an image (Celik, 2009; Chang & Yoon, 2003; Li & Yeh, 1998; Rodarmel & Shan, 2002).

#### Classification method: random forest

In this study, we developed three random forest (RF) models with different sets of input bands. RF is a machine learning algorithm that relies on an ensemble of uncorrelated decision trees to make a decision; trees are kept uncorrelated by using a bagging method in which decision trees randomly sample from a dataset (Breiman, 2001). RF classifiers have been widely used in remote sensing image classifications with high accuracy (Belgiu & Drăgu, 2016; Gislason et al., 2006; Pal, 2005; Rodriguez-Galiano et al., 2012). We used an RF classifier with 100 trees as a prior study indicated that more than 128 trees result in little to no performance gain (Oshiro et al., 2012). The remaining parameters were set to their default values in GEE as follows: variables per split=2 or 3 depending on the number of input variables (defaults to the square root of the number of variables); minimum leaf population=1, bag fraction = 0.5, out-of-bag mode = false, and seed 0 (random seed). The RF classifier used is from the Statistical Machine Intelligence and Learning Engine (SMILE) implemented in GEE. We compare three different RF models with different sets of input bands (Table 1). In the first RF model, we used the original four NAIP bands (red, green, blue, and NIR) as input into the classifier. In the second model, we used the four NAIP bands and the NDVI band. In the third RF model, we used the five NAIP-derived PCA bands as input (PCA 1, PCA 2, PCA 3, PCA 4, PCA 5).

We identified three landcover classes in our classification: *Phragmites*, other vegetation, and water. *Phragmites* represents any area covered by *Phragmites*. The "other vegetation" class covers all vegetation in the study area other than *Phragmites* (such as those listed in "Study area" section). The "water" class includes any pixels covered entirely by open water. *Phragmites* could be distinguished from other marsh vegetation due to its unique structure, making it appear different in color and texture from surrounding vegetation in the summertime NAIP images (Fig. 2a, b). We did not consider common land cover classes, such as forest or impervious surface, as these are rarely present within the estuarine wetlands of DE.

#### Variable importance

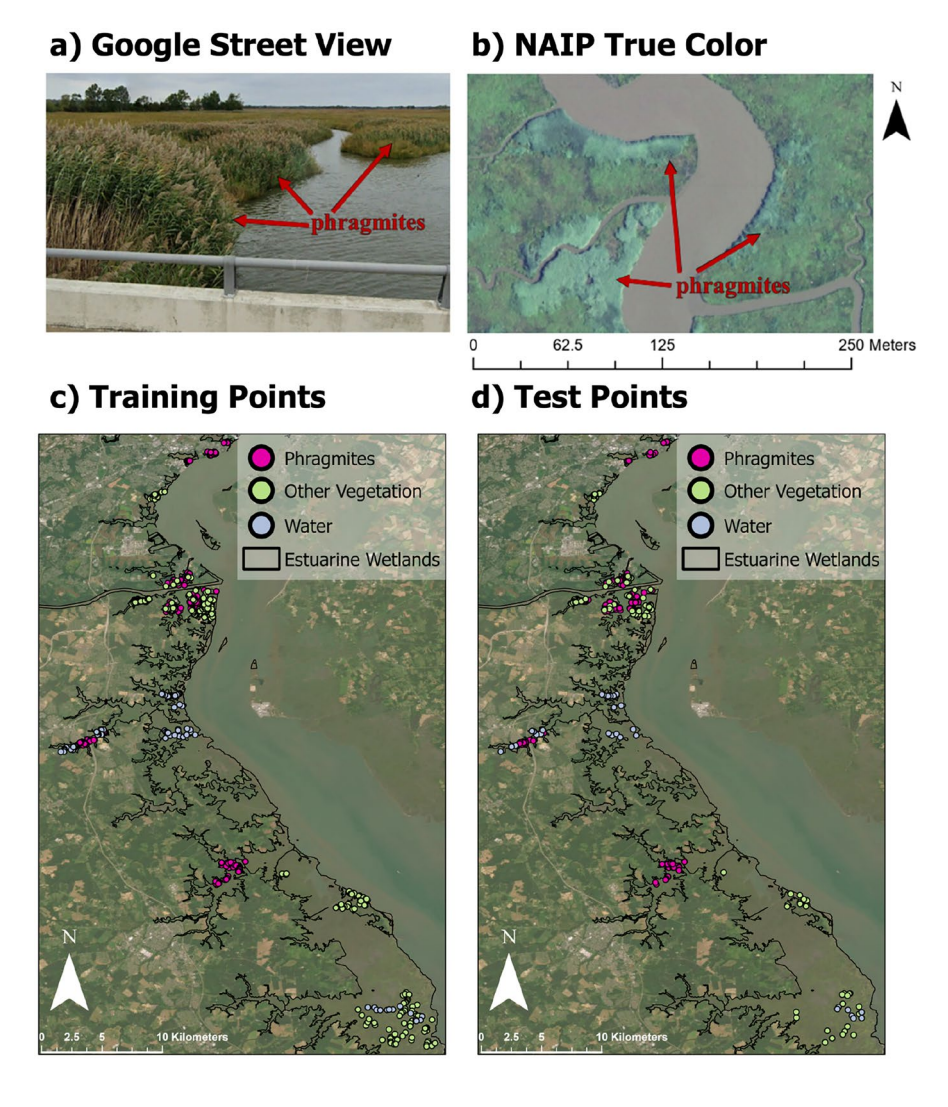
We calculated variable importance from the RF classification to determine which spectral bands are more effective in the classification of *Phragmites*. Variable importance is a measure of the influence that each individual input variable has on the output of a model. In remote sensing, the variable importance derived from RF land cover classifications has been used to identify the most relevant data (Belgiu & Drăgu, 2016). Two common methods used to measure variable importance from RF models are out-of-bag error and Gini impurity (Breiman, 2001; Breiman et al., 1984; Han et al., 2016). In this paper, variable importance was calculated as Gini impurity from the SMILE, in GEE (SMILE, 2022). Gini impurity-based importance measures the impurity each time a node is split. Impurity is the probability of incorrectly classifying a random sample in the dataset given that it was randomly labeled by the class distribution. The decrease in impurity is summed for each variable across each tree. The result of the Gini impurity is a single value for each input variable estimating the importance of that variable on the output of the model.

Table 1 Summary of all three RF model input bands

	Input bands			
Model 1	Red, green, blue, NIR			
Model 2	Red, green, blue, NIR, NDVI			
Model 3	PCA 1, PCA 2, PCA 3, PCA 4, PCA 5			



Fig. 2 Phragmites patches in an estuarine wetland as seen from a Google Street View and on a b NAIP true color image for the same location. Maps of all the collected reference points across three landcover classes for c training the machine learning classifier (70% of reference points) and d testing the accuracy of the classification (30% of reference points)



# Reference data

The initial set of reference data was collected in the field by recording point locations of *Phragmites* patches in estuarine wetlands within New Castle County, DE (Fig. 2c, d). Points were collected using the mobile application Epicollect5 by finding patches of *Phragmites* along roads and footpaths in New Castle and Kent County. One point was collected along the edge of each individual connected patch of *Phragmites*. These points were then adjusted to the center of the patch using the software ArcGIS Pro. Further reference points were collected by visual inspection of the NAIP aerial imagery and the PCA bands. Points collected through the visual assessment of the NAIP imagery were then verified

using Google Earth Pro's street view, which was effectively used to identify *Phragmites* patches that could be seen from the road. Reference points for 500 *Phragmites* and 400 other marsh plants were collected using this method. In addition, 150 water points were selected solely based on the NAIP imagery, resulting in a total of 1050 reference points that were then used for training and testing the RF classifier.

#### Accuracy assessment

An accuracy assessment was conducted to assess and compare the performance of each RF model. A total of 70% reference points (n=731; Phragmites=340, other vegetation=283, water=108) were used to train



the classifier, and 30% (n=319; Phragmites=160, other vegetation = 117, water = 42) were used to test the accuracy of the predictions. The accuracy of the classifications was assessed using an error matrix and kappa coefficient, a commonly used method in remote sensing image classification (Rwanga & Ndambuki, 2017). The total number of points that were correctly predicted was divided by the total number of test points to calculate the overall accuracy, an indicator of how closely the supervised classification matched human observations. A user's accuracy and the producer's accuracy were then calculated. The user's accuracy is calculated by dividing the number of correctly classified reference points in a single class by the total number of reference points being assigned to that class by the classifier. This represents an error of commission and is useful in determining how accurately each land cover is being classified. Producer's accuracy is the number of correctly classified reference points divided by the total number of reference points and reflects an error of omission. In addition, a kappa coefficient was calculated to evaluate the results of the classification in comparison to random guessing. (Cohen, 1960; Congalton, 1991).

**Table 2** Confusion matrices and accuracy assessments for both RF models

Classified points	Reference points				
	Phragmites	Other vegetation	Water	User's accuracy	Producer's accuracy
RF model 1					
Phragmites	151	8	0	95%	94%
Other vegetation	9	109	2	91%	93%
Water	0	0	40	100%	95%
Overall accuracy	94%				
Kappa	0.9				
RF model 2					
Phragmites	150	9	0	94%	94%
Other vegetation	9	109	2	91%	92%
Water	0	0	40	100%	95%
Overall accuracy	94%				
Kappa	0.89				
RF model 3					
Phragmites	154	5	0	97%	95%
Other vegetation	8	110	2	92%	96%
Water	0	0	40	100%	95%
Overall accuracy	95%				
Kappa	0.92				

#### Results

Effectiveness of NAIP for classifying *Phragmites* 

The overall accuracies for all three RF Models were greater than 90%, indicating that they all can be used to quantify Phragmites with confidence. RF model 1 using the four NAIP bands alone achieved a high overall accuracy of 94% and kappa of 0.90 (Table 2). RF model 2 with an NDVI band in addition to the four NAIP bands achieved a similar overall accuracy of 94% and slightly lower kappa of 0.89 compared to RF model 1. RF model 3 which utilized PCA bands only yielded the highest overall accuracy of 95% and a kappa coefficient of 0.92. The increase in overall accuracy between RF model 1 or 2 and 3 was due to an increase in the user's accuracy for the Phragmites class, increasing from 94-95 to 97% and an increase in producer's accuracy for the other vegetation class, which increased from 92-93 to 96%. When classifying marshes dominated by *Phragmites*, all three models tended to yield similar results (Fig. 3a-d). Differences in model output can better be observed in marshes dominated by plants other than *Phragmites*,



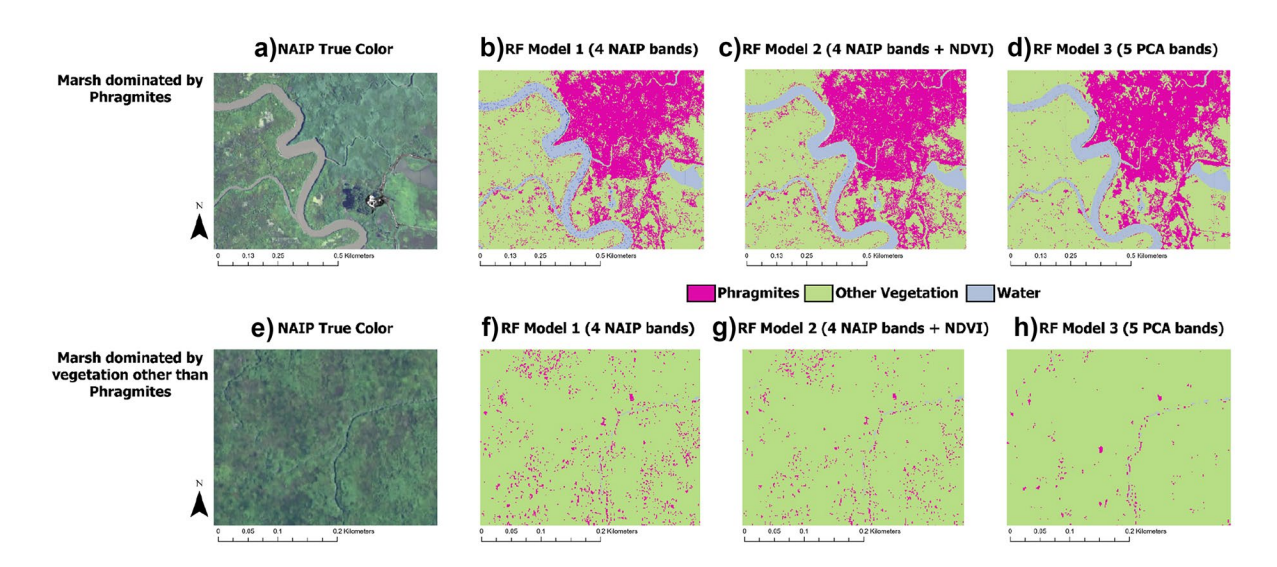


**Fig. 3** Comparison of results from the three RF models for a marsh dominated by *Phragmites* (**a**–**d**) and a marsh dominated by other vegetation (**e**–**h**). **a**, **e** visualize the red, green, and blue bands from the NAIP which are used as input into the model, **b**, **f** show results from RF model 1 which uses the four original

NAIP bands, **c**, **g** show results from RF model 2 which use the four NAIP bands and an NDVI band, and **d**, **h** show the results from RF model 3 which uses five PCA bands derived from the NAIP and NDVI bands

where model 1 and model 2 overpredict the *Phrag-mites* class compared to model 3 (Fig. 3e–h). To quantify the extent of *Phragmites* in DE, the output from RF model 3 was used due to its higher overall accuracy, kappa, user's accuracy for the *Phragmites* class, and decreased likelihood to overpredict *Phragmites*.

Monthly NDVI data from Sentinel-2 in 2017 reveals that the spectral signature of *Phragmites* is the most distinct from other vegetation and water during June and July (Fig. 4). Moreover, the NDVI values of *Phragmites* are distinct from those of other vegetation throughout the months of May through October, thus justifying the use of summer and early fall NAIP images in *Phragmites* identification.

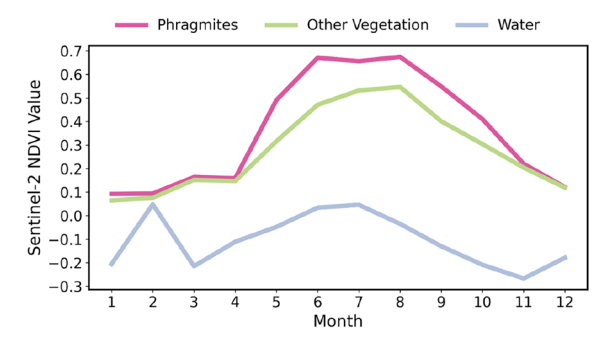


Fig. 4 Monthly NDVI values for the three land cover classes for 2017

# Variable importance of NDVI and PCA bands

The NIR band has the highest variable importance in RF model 1 (Fig. 5a) followed by the blue band. In RF model 2, the NDVI band has the highest variable importance, followed by the blue band (Fig. 5b). In RF model 3, the PCA 1 band has the highest importance followed by PCA 3 (Fig. 5c). The histograms in Fig. 6 show the pixel values for the classified points across all ten NAIP-derived bands used in this study with notable differences observed for different bands. For example, the pixel values of PCA 1 and 3 for the *Phragmites* class are higher than the values for the other vegetation and water classes (Fig. 6h), resulting in separable spectral clusters. Conversely, the red band's pixel values show little separation between *Phragmites* and other vegetation (Fig. 6b).

## Spatial extent of Phragmites in DE

Our findings indicate that *Phragmites* is widespread throughout DE; however, there are spatial variations between counties. We estimate that 11% of the estuarine wetland area in DE is covered by *Phragmites*, totaling 52 km<sup>2</sup> (Fig. 7a). Of DE's three counties, New Castle has the highest percentage of estuarine wetlands covered by *Phragmites* at 17% (Fig. 7c), while having the least



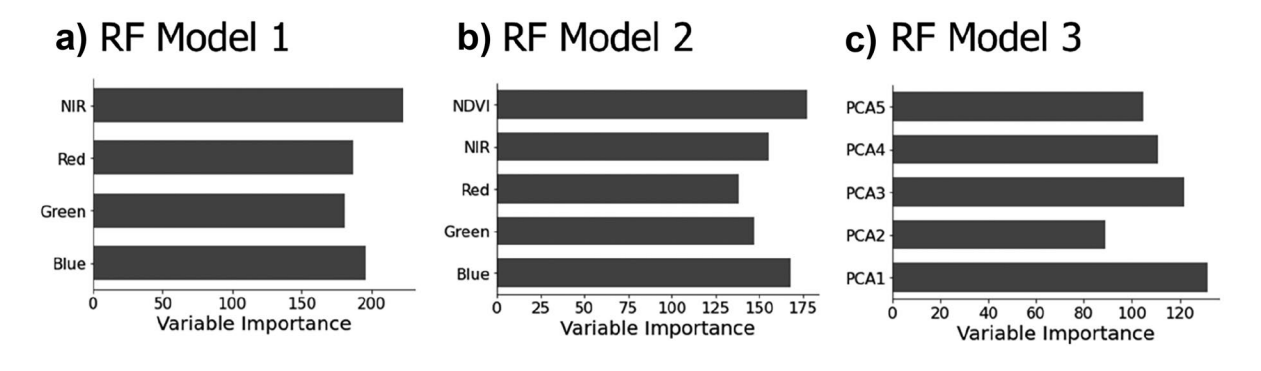


Fig. 5 The variable importance of each input band used in all three RF models using Gini impurity. Higher values for an input band indicate higher importance of that band in increasing classification accuracy

area covered by *Phragmites* at 15 km<sup>2</sup> (Fig. 7b). Kent County has the second highest percentage of estuarine wetlands covered in *Phragmites* at 11% while also having the highest area covered by *Phragmites* at 19 km<sup>2</sup>.

Finally, Sussex County has the lowest percentage of estuarine wetlands covered by *Phragmites* at 9%, totaling 17 km<sup>2</sup>.

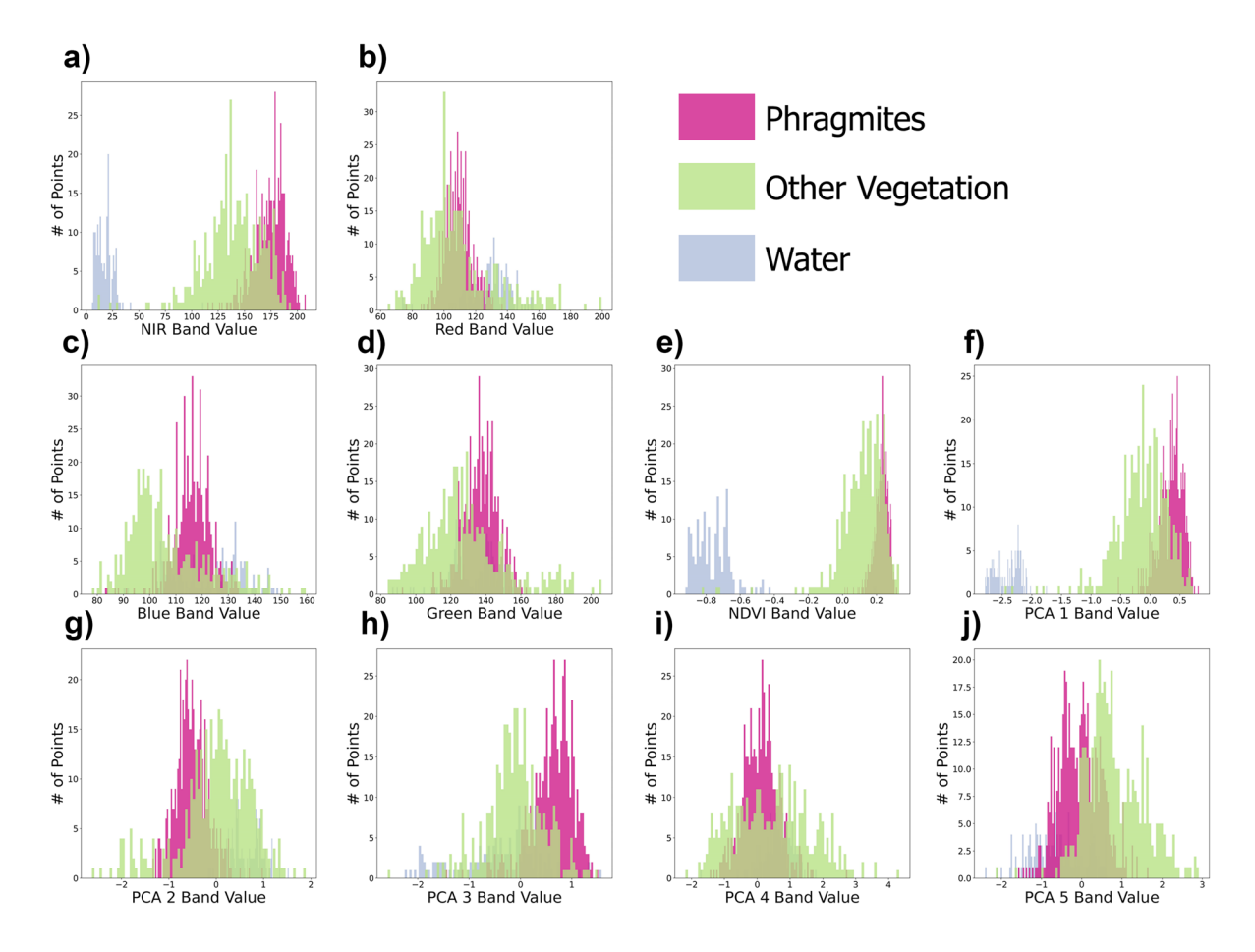
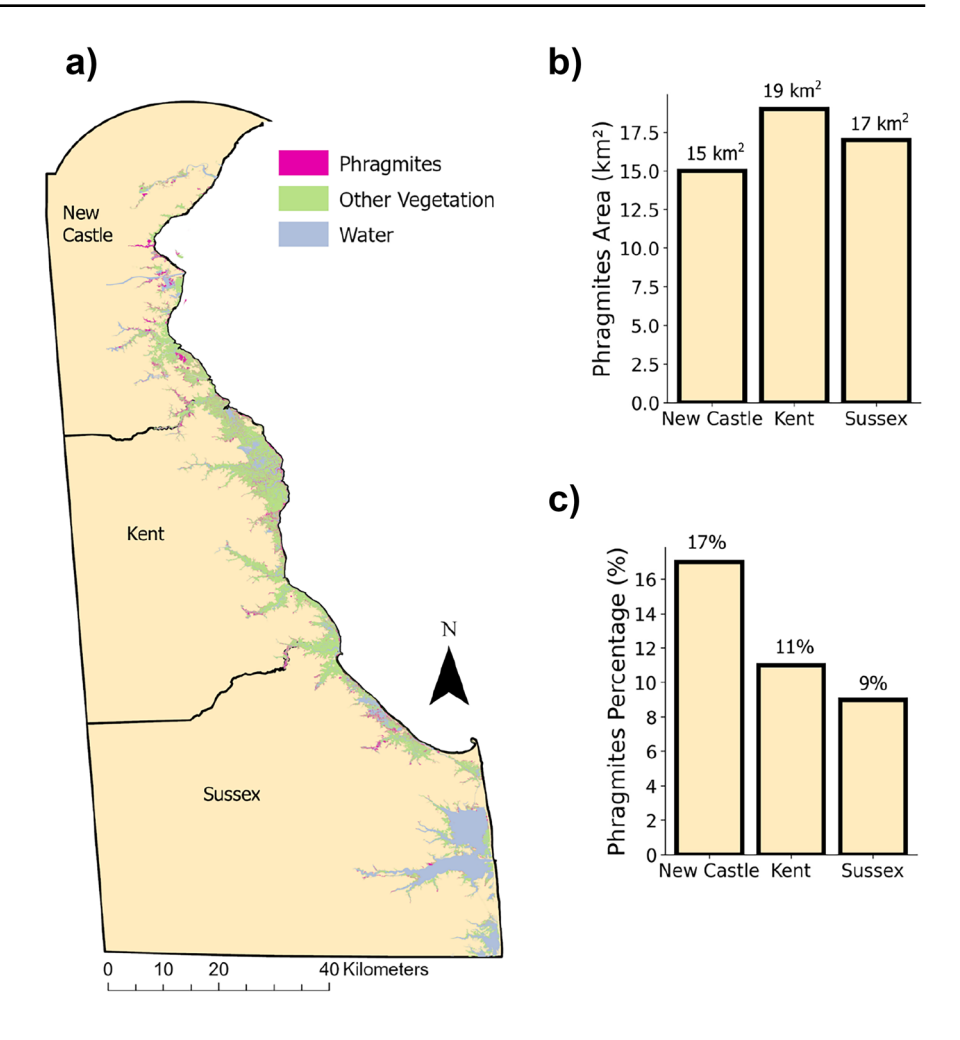


Fig. 6 Histograms of the digital values for pixels in each input band from the NAIP, NDVI, and PCA grouped by the manual classification of the land cover classified for that pixel (*Phragmites*, other vegetation, or water)



Fig. 7 Classification results from the most accurate RF model, RF model 3. The left panel shows the spatial distribution of *Phragmites* in the classified land cover image (a). Right panels show the total area under the *Phragmites* class in each DE county (b) and the percentage of classified wetland areas covered by *Phragmites* (c)

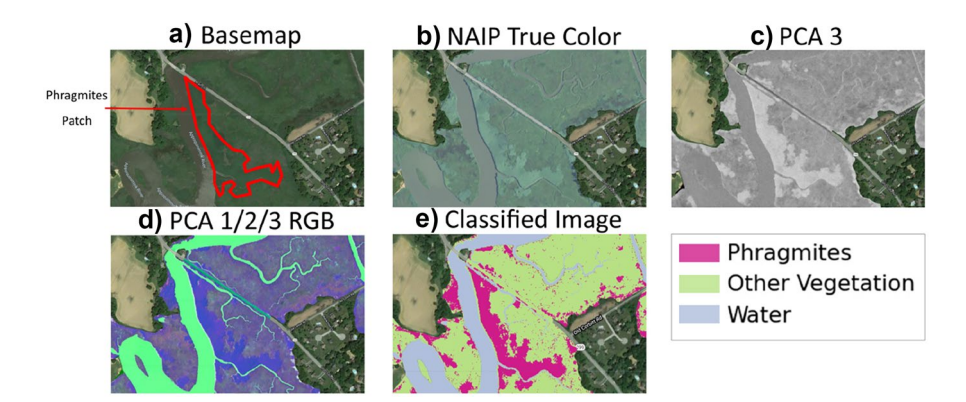


# Discussion

In this study, we achieved an overall high accuracy of 94%–95% in classifying *Phragmites*, irrespective of the NAIP-derived input bands used. However, the mapping of *Phragmites* using remote sensing presents several challenges, such as those stemming from similar spectral signatures between Phragmites and other marsh vegetation and the large diversity of marsh vegetation creating overlapping spectral signatures. Despite having limited spectral and seasonal information, NAIP images from the summer of 2017 provided sufficient details for *Phragmites* to be visually distinguishable from other vegetation within DE's estuarine wetlands. Phragmites patches have a distinct color and texture, primarily due to their distinct values in the blue and NIR portions of the electromagnetic spectrum compared to other marsh vegetation in the surrounding areas (Fig. 6). The spectral separation of *Phragmites* from other vegetation and water was greatest during summer months, meaning that NAIP data which is typically collected during summer is an effective source for mapping *Phragmites*. This result is consistent with another study which found that the separability of *Phragmites* from most other vegetation types was greatest during July based on multispectral moderate-resolution satellite data (Rupasinghe & Chow-Fraser, 2019).

The NAIP data provides a clear visual distinction between the three land cover classes (*Phragmites*, other vegetation, and water) (Fig. 8a, b). The first three PCA-derived NAIP bands also show this distinction (*Phragmites*, other vegetation, and water), with *Phragmites* appearing in a darker color compared to the surrounding vegetation (Fig. 8d). This aligns with prior research that has concluded that the first few PCA bands of a remotely sensed image generally reduce noise compared





to the final components (Fung & LeDrew, 1987). This visual distinction is most evident in the PCA 3 band, which demonstrates a sharp contrast between the *Phragmites* and surrounding vegetation, as *Phragmites* appears in bright whitish color compared to the darker gray of other vegetation and water (Fig. 8c). Thus, classified images from 1 year with such distinct separability between *Phragmites* and other vegetation from the PCA 3 band can facilitate effective "on-the-screen" collection of large volumes of reference data to train and test machine learning models for other years, minimizing the need for in situ data collection on an annual basis.

The user's accuracy for *Phragmites* of 97% obtained through the use of NAIP bands, NDVI, and PCA is comparable to or higher than those achieved in prior studies using other remote sensing methods for mapping Phragmites. For example, Bourgeau-Chavez et al. (2013) and Bourgeau-Chavez et al. (2015) used synthetic aperture radar (SAR) to map Phragmites with a user's accuracy of 43% and 64% respectively. Pengra et al. (2007) mapped Phragmites with a user's accuracy of 61.1% using hyperspectral remote sensing. Samiappan et al. (2016) and Abeysinghe et al. (2019) achieved a high user's accuracy for *Phragmites* mapping (between 94 and 99% at different sites) through the use of high-resolution imagery captured by an unmanned aerial system (UAS) and computed bands such as a gray-level co-occurrence matrix (GLCM), NDVI, and canopy height model (CHM). This paper presents a method with comparable accuracy, and the use of freely accessible NAIP data with coverage across the USA on a cloud computing platform, thus making it more affordable in terms of cost, time, and computational power. A similar NAIP-based classification of *Phragmites* that utilized the four NAIP bands (red, green, blue, and near-infrared) and multiple wetland plant species as output classes achieved a user's accuracy of 85% and a producer's accuracy of 85-99% for *Phragmites* (Xie et al., 2015). Our results showed that including an NDVI band (calculated using red and NIR bands) does not drastically change classification accuracy because similar information is already included through the direct use of the red and NIR bands as classifier inputs. The use of PCA leads to slightly more accurate results. The high accuracy of this method in addition to the large spatial coverage of input data makes it suitable for identifying Phragmites invasions for control efforts in estuarine wetlands in the northeastern USA at a state-wide level. Because of the regular release of new NAIP data, with imagery being collected for half of the USA every year, this method also enables the regular monitoring of *Phragmites*. Frequent monitoring is essential for *Phragmites* which has the ability to spread rapidly in marsh areas undergoing land-use conversions (Jodoin et al., 2008; Rice et al., 2000; Saltonstall, 2002). Such frequent monitoring can inform and improve management efforts to mitigate the negative impacts associated with *Phragmites* invasions such as a loss of biodiversity, hydrological alterations, and changes in ecosystem functioning (Meyerson et al., 2009).

While this method achieves a high overall accuracy, classification error still exists, mainly from misclassification between *Phragmites* and other vegetation. While the use of PCA bands reduced the misclassification of *Phragmites*, classification uncertainty often stems from the wide diversity of marsh plants. Across a large study area, even relatively small amounts of misclassifications may compound and lead to imperfect estimates of the total land area under *Phragmites*. Future research may benefit from determining which plant types are most commonly being confused for *Phragmites* and better training the classifier for these plant types in order to reduce classification errors.



Based on our classification, Phragmites makes up a higher percentage of the estuarine wetland area in New Castle County when compared to DE's other two counties. New Castle is also the most urbanized county in DE, with 31% of its area being comprised of impervious land cover compared to 9% in both Kent and Sussex County (Walter & Mondal, 2019). This result is consistent with other studies on the spread of Phragmites, which have shown increased spread in areas with more urban and suburban land uses (King et al., 2007; McCormick et al., 2010; Tulbure & Johnston, 2010). Research in the Chesapeake Bay found that *Phragmites* invasions were highly correlated with shoreline agriculture based on visual assessments between 2001 and 2005 (Chambers et al., 2008). However, we find that Kent County has the lowest percentage of *Phragmites* in 2017 while having the highest percentage of cropland at 49% compared to 45% in Sussex and 30% in New Castle (Walter & Mondal, 2019).

Our results show that Phragmites makes up a large portion of DE's estuarine ecosystems, covering 11% of all estuarine wetlands throughout the state. Climate change-induced saltwater intrusion has already begun to affect soil chemistry in the Eastern USA creating new habitat for *Phragmites* (Smith, 2013; Tully et al., 2019). The invasion of *Phragmites* has been observed in areas of forest-marsh transition caused by saltwater intrusion, leading to the degradation of wildlife habitat (Taylor et al., 2020). The rate of saltwater intrusion is likely to increase over the next decades as the rate of sea level rise increases; projections estimate 0.25–0.30 m of sea level rise along the USA coastline by 2050, the same level of increase as seen between 1920 and 2020 (Sweet et al., 2022). As anthropogenically induced conditions continue to reshape our land and provide new opportunities for *Phragmites* invasions, the effective control of *Phragmites* will have increasing importance in ecosystem management.

#### **Conclusions**

This study demonstrates the ability to classify *Phragmites* on a state-wide geographic scale within estuarine wetland environments. This method is easy and cost-effective to reproduce as it utilizes the freely available NAIP dataset provided by the USDA and GEE code that has been made publicly available. The use of PCA on the original NAIP bands and NDVI as an input into the RF

model led to higher overall classification accuracy (95%) than that achieved through the use of the four original NAIP bands alone (94%). However, classification based on the original four NAIP bands might provide a simpler option for land managers. Utilizing remote sensing to map *Phragmites* in estuaries at the state level, especially in coastal states such as DE, can create a useful inventory of where *Phragmites* is growing. This may be useful information for programs such as the *Phragmites* control cost-share program run by the Delaware Division of Fish and Wildlife which aims to control the spread of Phragmites. Through the use of NAIP data, there is the potential to map *Phragmites* at 2- to 3-year intervals. By creating biennial or triennial geospatial datasets in the future, the spread of *Phragmites* can be monitored to understand how effectively the spread is being managed.

**Acknowledgements** We thank the reviewers for their constructive criticism of an earlier version of this manuscript. We thank Bruce Vasilas for his guidance in the field.

Author contribution Conceptualization: Matthew Walter. Methodology: Matthew Walter and Pinki Mondal. Writing—original draft preparation: Matthew Walter. Writing—review and editing: Pinki Mondal. Funding acquisition: Matthew Walter and Pinki Mondal.

**Funding** This publication was made possible by the National Science Foundation EPSCoR grant no. 1757353 and the State of Delaware. This work was also supported by the NASA EPSCoR grant (DE-80NSSC20M0220). The lead author was supported by the NASA Delaware Space Grant College and Fellowship Program (80NSSC20M0045).

**Data availability** The classified Phragmites dataset from model 3 generated for this article is available through Zenodo at https://zenodo.org/record/7644496. The GEE code used for the classification of Phragmites from NAIP imagery is available at https://github.com/mattswalter/Phragmites\_Classification.

#### **Declarations**

**Competing interests** The authors declare no competing interests.

#### References

Abeysinghe, T., Simic Milas, A., Arend, K., Hohman, B., Reil, P., Gregory, A., & Vázquez-Ortega, A. (2019). Mapping Invasive Phragmites australis in the Old Woman Creek Estuary Using UAV Remote Sensing and Machine Learning Classifiers. *Remote Sensing*, 11(11), 1380. https://doi.org/10.3390/rs11111380

Anderson, C. J., Heins, D., Pelletier, K. C., Bohnen, J. L., & Knight, J. F. (2021). Mapping Invasive Phragmites australis



- Using Unoccupied Aircraft System Imagery, Canopy Height Models, and Synthetic Aperture Radar. *Remote Sensing*, 13(16), 3303. https://doi.org/10.3390/RS13163303
- Avers, B., Fahlsing, R., Kafcas, E., Schafer, T., Collin, T., Esman, L., & Scheun, D. (2014). A Guide to the Control and Management of Invasive Phragmites.
- Basu, S., Ganguly, S., Nemani, R. R., Mukhopadhyay, S., Zhang, G., Milesi, C., & Li, S. (2015). A Semiautomated Probabilistic Framework for Tree-Cover Delineation From 1-m NAIP Imagery Using a High-Performance Computing Architecture. *IEEE Transactions on Geoscience and Remote Sensing*, 53(10), 5690–5708. https://doi.org/10. 1109/TGRS.2015.2428197
- Belgiu, M., & Drăgu, L. (2016). Random forest in remote sensing: A review of applications and future directions. ISPRS Journal of Photogrammetry and Remote Sensing, 114, 24–31. https://doi.org/10.1016/J.ISPRSJPRS.2016.01.011
- Benoit, L. K., & Askins, R. A. (1999). Impact of the spread of Phragmites on the distribution of birds in Connecticut tidal marshes. Wetlands, 19(1), 194–208. https://doi.org/10.1007/ BF03161749
- Bertelsmeier, C., Luque, G. M., & Courchamp, F. (2013). Increase in Quantity and Quality of Suitable Areas for Invasive Species as Climate Changes. *Conservation Biology*, 27(6), 1458–1467. https://doi.org/10.1111/COBI.12093
- Bolton, R. M., & Brooks, R. J. (2010). Impact of the Seasonal Invasion of Phragmites australis (Common Reed) on Turtle Reproductive Success. *Chelonian Conservation and Biology*, 9(2), 238–243. https://doi.org/10.2744/CCB-0793.1
- Bourgeau-Chavez, L. L., Kowalski, K. P., Carlson Mazur, M. L., Scarbrough, K. A., Powell, R. B., Brooks, C. N., & Riordan, K. (2013). Mapping invasive Phragmites australis in the coastal Great Lakes with ALOS PALSAR satellite imagery for decision support. *Journal of Great Lakes Research*, 39(S1), 65–77. https://doi.org/10.1016/J.JGLR.2012.11.001
- Bourgeau-Chavez, L., Endres, S., Battaglia, M., Miller, M. E., Banda, E., Laubach, Z., Higman, P., Chow-Fraser, P., & Marcaccio, J. (2015). Development of a Bi-National Great Lakes Coastal Wetland and Land Use Map Using Three-Season PALSAR and Landsat Imagery. *Remote Sensing*, 7(7), 8655–8682. https://doi.org/10.3390/RS70708655
- Bradley, B. A., Blumenthal, D. M., Early, R., Grosholz, E. D., Lawler, J. J., Miller, L. P., & Olden, J. D. (2012). Global change, global trade, and the next wave of plant invasions. *Frontiers in Ecology and the Environment*, 10(1), 20–28. https://doi.org/10.1890/110145
- Breiman, L. (2001). Random Forests. *Machine Learning*, 45(1), 5–32. https://doi.org/10.1023/A:1010933404324
- Breiman, L., Friedman, J. H., Olshen, R. A., & Stone, C. J. (1984). Classification and regression trees. In Classification and Regression Trees. https://doi.org/10.1201/9781315139 470/CLASSIFICATION-REGRESSION-TREES-LEO-BREIMAN-JEROME-FRIEDMAN-RICHARD-OLSHEN-CHARLES-STONE
- Celik, T. (2009). Unsupervised change detection in satellite images using principal component analysis and κ-means clustering. *IEEE Geoscience and Remote Sensing Letters*, 6(4), 772–776. https://doi.org/10.1109/LGRS.2009.2025059
- Chambers, R. M., Havens, K. J., Killeen, S., & Berman, M. (2008). Common reed Phragmites australis occurrence and adjacent land use along estuarine shoreline in

- Chesapeake Bay. *Wetlands*, 28(4), 1097–1103. https://doi.org/10.1672/07-61.1
- Chambers, R. M., Meyerson, L. A., & Saltonstall, K. (1999). Expansion of Phragmites australis into tidal wetlands of North America. *Aquatic Botany*, 64(3–4), 261–273. https://doi.org/10.1016/S0304-3770(99)00055-8
- Chang, H., & Yoon, W. S. (2003). Improving the classification of Landsat data using standardized principal components analysis. KSCE Journal of Civil Engineering, 7(4), 469– 474. https://doi.org/10.1007/bf02895842
- Cohen, J. (1960). A Coefficient of Agreement for Nominal Scales. *Educational and Psychological Measurement*, 20(1), 37–46. https://doi.org/10.1177/001316446002000104
- Congalton, R. G. (1991). A review of assessing the accuracy of classifications of remotely sensed data. *Remote Sensing of Environment*, 37(1), 35–46. https://doi.org/10.1016/0034-4257(91)90048-B
- Correll, M. D., Hantson, W., Hodgman, T. P., Cline, B. B., Elphick, C. S., Gregory Shriver, W., & Olsen, B. J. (2019). Fine-Scale Mapping of Coastal Plant Communities in the Northeastern USA. Wetlands, 39(1), 17–28. https://doi. org/10.1007/S13157-018-1028-3/FIGURES/4
- Davies, K. W., Petersen, S. L., Johnson, D. D., Davis, D. B., Madsen, M. D., Zvirzdin, D. L., & Bates, J. D. (2010). Estimating juniper cover from national agriculture imagery program (NAIP) imagery and evaluating relationships between potential cover and environmental variables. *Rangeland Ecology and Management*, 63(6), 630–637. https://doi.org/ 10.2111/REM-D-09-00129.1
- Diagne, C., Leroy, B., Vaissière, A. C., Gozlan, R. E., Roiz, D., Jarić, I., & Courchamp, F. (2021). High and rising economic costs of biological invasions worldwide. *Nature*, 592(7855), 571–576. https://doi.org/10.1038/s41586-021-03405-6
- DNREC. (2022). Private Lands Assistance. Retrieved April 25, 2022, from https://dnrec.alpha.delaware.gov/fish-wildlife/ conservation/private-lands/
- Ehrenfeld, J. G. (2010). Ecosystem Consequences of Biological Invasions. Annual Review of Ecology, Evolution, and Systematics, 41, 59–80. https://doi.org/10.1146/ANNUREV-ECOLSYS-102209-144650
- Fung, T., & LeDrew, E. (1987). Application of principal components analysis to change detection. *Photogrammetric Engineering and Remote Sensing*, 53(12), 1649–1658. Retrieved from <a href="https://www.semanticscholar.org/paper/Application-of-principal-components-analysis-to-Fung-LeDrew/107efa1cdccbe3650fbc0bc0fd374e65a24c5bbf">https://www.semanticscholar.org/paper/Application-of-principal-components-analysis-to-Fung-LeDrew/107efa1cdccbe3650fbc0bc0fd374e65a24c5bbf</a>
- Gedan, K. B., & Fernández-Pascual, E. (2019). Salt marsh migration into salinized agricultural fields: A novel assembly of plant communities. *Journal of Vegetation Science*, 30(5), 1007–1016. https://doi.org/10.1111/JVS.12774
- GEE. (2022). Eigen Analysis. Retrieved from https://developers. google.com/earth-engine/arrays\_eigen\_analysis
- Gislason, P. O., Benediktsson, J. A., & Sveinsson, J. R. (2006). Random forests for land cover classification. *Pattern Recognition Letters*, 27(4), 294–300. https://doi.org/10.1016/j.patrec.2005.08.011
- Gorelick, N., Hancher, M., Dixon, M., Ilyushchenko, S., Thau, D., & Moore, R. (2017). Google Earth Engine: Planetary-scale geospatial analysis for everyone. *Remote Sensing of Environment*, 202, 18–27. https://doi.org/10.1016/j.rse.2017.06.031



- Hayes, M. M., Miller, S. N., & Murphy, M. A. (2014). Highresolution landcover classification using Random Forest. *Remote Sensing Letters*, 5(2), 112–121. https://doi.org/10. 1080/2150704X.2014.882526
- Hazelton, E. L. G., Mozdzer, T. J., Burdick, D. M., Kettenring, K. M., & Whigham, D. F. (2014). Phragmites australis management in the United States: 40 years of methods and outcomes. AoB PLANTS, 6. https://doi.org/10.1093/AOBPLA/PLU001
- Hellmann, J. J., Byers, J. E., Bierwagen, B. G., & Dukes, J. S. (2008). Five Potential Consequences of Climate Change for Invasive Species. *Conservation Biology*, 22(3), 534– 543. https://doi.org/10.1111/J.1523-1739.2008.00951.X
- Hogland, J., Anderson, N., & St. Peter, J., Drake, J., & Medley, P. (2018). Mapping Forest Characteristics at Fine Resolution across Large Landscapes of the Southeastern United States Using NAIP Imagery and FIA Field Plot Data. ISPRS International Journal of Geo-Information, 7(4), 140. https://doi.org/10.3390/ijgi7040140
- Jodoin, Y., Lavoie, C., Villeneuve, P., Theriault, M., Beaulieu, J., & Belzile, F. (2008). Highways as corridors and habitats for the invasive common reed Phragmites australis in Quebec. *Canada. Journal of Applied Ecology*, 45(2), 459– 466. https://doi.org/10.1111/j.1365-2664.2007.01362.x
- Jolliffe, I. T., & Cadima, J. (2016). Principal component analysis: A review and recent developments. *Philosophical Transactions of the Royal Society A: Mathematical, Physical and Engineering Sciences*, 374(2065), 20150202. https://doi.org/10.1098/rsta.2015.0202
- Kettenring, K. M., Blois, S. de, & Hauber, D. P. (2012). Moving from a regional to a continental perspective of Phragmites australis invasion in North America. AoB Plants. https:// doi.org/10.1093/AOBPLA/PLS040
- King, R. S., Deluca, W. V., Whigham, D. F., & Marra, P. P. (2007). Threshold effects of coastal urbanization on Phragmites australis (common reed) abundance and foliar nitrogen in Chesapeake Bay. *Estuaries and Coasts* 30(3), 469– 481. https://doi.org/10.1007/BF02819393
- Li, X., & Yeh, A. G. O. (1998). Principal component analysis of stacked multi-temporal images for the monitoring of rapid urban expansion in the Pearl River Delta. *International Journal of Remote Sensing*, 19(8), 1501–1518. https://doi.org/10.1080/014311698215315
- Li, X., Myint, S. W., Zhang, Y., Galletti, C., Zhang, X., & Turner, B. L. (2014). Object-based land-cover classification for metropolitan Phoenix, Arizona, using aerial photography. *International Journal of Applied Earth Observation and Geoinformation*, 33(1), 321–330. https://doi.org/10.1016/j.jag.2014.04.018
- Linders, T. E. W., Schaffner, U., Eschen, R., Abebe, A., Choge, S. K., Nigatu, L., & Allan, E. (2019). Direct and indirect effects of invasive species: Biodiversity loss is a major mechanism by which an invasive tree affects ecosystem functioning. *Journal of Ecology*, 107(6), 2660–2672. https://doi.org/10.1111/1365-2745.13268
- Liu, H., Meng, X., Jiang, T., Liu, X., & Zhang, A. (2016a). Change Detection of Phragmites Australis Distribution in

- the Detroit Wildlife Refuge Based on an Iterative Intersection Analysis Algorithm. *Sustainability*, 8(3), 264. https://doi.org/10.3390/SU8030264
- Liu, X., Zhang, A., Wang, H., & Liu, H. (2016b). Using multiremote sensing data to assess Phragmites invasion of the Detroit river international wildlife refuge. World Journal of Engineering, 13(1), 44–52. https://doi.org/10.1108/WJE-02-2016-016/FULL/XML
- Mal, T. K., & Narine, L. (2004). The biology of Canadian weeds. 129. Phragmites australis (Cav.) Trin. ex Steud. *Canadian Journal of Plant Science*, 84(1), 365–396. https://doi.org/10.4141/P01-172
- Marks, M., Lapin, B., & Randall, J. (1994). Phragmites australis (P. communis): threats, management and monitoring. Natural Areas Journal, 14(4), 285–294.
- Martin, L. J., & Blossey, B. (2013). The Runaway Weed: Costs and Failures of Phragmites australis Management in the USA. *Estuaries and Coasts*, *36*(3), 626–632. https://doi.org/10.1007/S12237-013-9593-4/TABLES/3
- Maxwell, A. E., Warner, T. A., Vanderbilt, B. C., & Ramezan, C. A. (2017). Land Cover Classification and Feature Extraction from National Agriculture Imagery Program (NAIP) Orthoimagery: A Review. *Photogrammetric Engineering and Remote Sensing*, 83(11), 737–747. https://doi.org/10.14358/PERS.83.10.737
- McCormick, M. K., Kettenring, K. M., Baron, H. M., & Whigham, D. F. (2010). Extent and reproductive mechanisms of phragmites australis spread in brackish wetlands in Chesapeake bay, Maryland (USA). Wetlands, 30(1), 67–74. https://doi.org/10.1007/S13157-009-0007-0/FIGURES/2
- Meyerson, L., Saltonstall, K., & Chambers, R. (2009). Phragmites australis in Eastern North America: A Historical and Ecological Perspective. In B. Silliman, E. Grosholz, & M. Bertness (Eds.), *Human Impacts on Salt Marshes: A Global Perspective*. Retrieved from https://books.google.com/books?hl=en&lr=&id=Vs-IDwAAQBAJ&oi=fnd&pg=PA57&dq=impacts+of+phragmites+invasion&ots=eJIxH\_rkfr&sig=81eoEzB0KfZRoRs6Dza4fUBZtB8#v=onepage&q=impactsofphragmites invasion&f=false
- Minchinton, T. E., & Bertness, M. D. (2003). Disturbancemediated competition and the spread of Phragmites australis in a coastal marsh. *Ecological Applications*, 13(5), 1400–1416. https://doi.org/10.1890/02-5136
- Misra, G., Cawkwell, F., & Wingler, A. (2020). Status of Phenological Research Using Sentinel-2 Data: A Review. Remote Sensing, 12(17), 2760. https://doi.org/10.3390/RS12172760
- Nagel, P., & Yuan, F. (2016). High-resolution land cover and impervious surface classifications in the twin cities metropolitan area with NAIP Imagery. *Photogrammetric Engi*neering and Remote Sensing, 82(1), 63–71. https://doi.org/ 10.14358/PERS.83.1.63
- NAIP. (2012). National Agriculture Imagery Program (NAIP).

  National Agriculture Imagery Program (NAIP) Information
  Sheet. Retrieved from https://www.fsa.usda.gov/Internet/
  FSA\_File/naip\_info\_sheet\_2013.pdf
- NWI. (1985). Wetlands of Delaware.
- Oshiro, T. M., Perez, P. S., & Baranauskas, J. A. (2012). How many trees in a random forest? Lecture Notes in Computer Science (Including Subseries Lecture Notes in Artificial Intelligence and Lecture Notes in Bioinformatics). LNAI, 7376, 154–168. https://doi.org/10.1007/978-3-642-31537-4\_13



- Pal, M. (2005). Random forest classifier for remote sensing classification. *International Journal of Remote Sensing*, 26(1), 217–222. https://doi.org/10.1080/01431160412331269698
- Pearson, K. (1901). LIII. On lines and planes of closest fit to systems of points in space. The London, Edinburgh, and Dublin Philosophical Magazine and Journal of Science, 2(11), 559–572. https://doi.org/10.1080/14786440109462720
- Pengra, B. W., Johnston, C. A., & Loveland, T. R. (2007). Mapping an invasive plant, Phragmites australis, in coastal wetlands using the EO-1 Hyperion hyperspectral sensor. *Remote Sensing of Environment*, 108(1), 74–81. https://doi.org/10.1016/J.RSE.2006.11.002
- Reichard, S., & White, P. (2001). Horticulture as a Pathway of Invasive Plant Introductions in the United States: Most invasive plants have been introduced for horticultural use by nurseries, botanical gardens, and individuals. *BioScience*, 51(2), 103–113. https://academic.oup.com/bioscience/article/51/2/ 103/390610
- Rice, D., Rooth, J., & Stevenson, J. (2000). Colonization and expansion of Phragmites australis in upper Chesapeake Bay tidal marshes. Wetlands, 20(280). Retrieved from https://doi.org/10.1672/0277-5212(2000)020[0280:CAE-OPA]2.0.CO;2
- Robichaud, C. D., & Rooney, R. C. (2017). Long-term effects of a Phragmites australis invasion on birds in a Lake Erie coastal marsh. *Journal of Great Lakes Research*, 43(3), 141–149. https://doi.org/10.1016/J.JGLR.2017.03.018
- Rodarmel, C., & Shan, J. (2002). Principal Component Analysis for Hyperspectral Image Classification. In *Information Systems* (Vol. 62).
- Rodriguez-Galiano, V. F., Ghimire, B., Rogan, J., Chica-Olmo, M., & Rigol-Sanchez, J. P. (2012). An assessment of the effectiveness of a random forest classifier for land-cover classification. *ISPRS Journal of Photogrammetry and Remote Sensing*, 67(1), 93–104. https://doi.org/10.1016/j.isprsjprs.2011.11.002
- Rouse, J., Haas, R. H., Schell, J. A., & Deering, D. (1974). Monitoring vegetation systems in the great plains with ERTS. NASA. Goddard Space Flight Center 3d ERTS-1 Symp., Vol. 1, Sect. A.
- Rupasinghe, P. A., & Chow-Fraser, P. (2019). Identification of most spectrally distinguishable phenological stage of invasive Phramites australis in Lake Erie wetlands (Canada) for accurate mapping using multispectral satellite imagery. Wetlands Ecology and Management, 27(4), 513–538. https:// doi.org/10.1007/S11273-019-09675-2/FIGURES/9
- Rwanga, S. S., & Ndambuki, J. M. (2017). Accuracy Assessment of Land Use/Land Cover Classification Using Remote Sensing and GIS. *International Journal of Geosciences*, 08(04), 611–622. https://doi.org/10.4236/ijg.2017.84033
- Saltonstall, K. (2002). Cryptic invasion by a non-native genotype of the common reed, Phragmites australis, into North America. Proceedings of the National Academy of Sciences of the United States of America, 99(4), 2445–2449. https://doi.org/10.1073/PNAS.032477999/ASSET/5887847F-C0C8-4861-B366-1379B9EA1738/ASSETS/GRAPHIC/PQ0324779003.JPEG
- Saltonstall, K. (2003). Genetic variation among North American populations of Phragmites australis: Implications for management. *Estuaries*, 26(2), 444–451.https://doi.org/10.1007/BF02823721

- Saltonstall, K., Peterson, P., & Soreng, R. (2004). Recognition ecognition of phragmites au straus subsp. Americanus (Poaceae: arundinoideae) in North America: evidence from morphologicaL and genetic analyses on jstor. SIDA, Contributions to Botany, 21(2), 683–692. Retrieved from https:// www.jstor.org/stable/41968310
- Samiappan, S., Turnage, G., Hathcock, L., Casagrande, L., Stinson, P., & Moorhead, R. (2016). Using unmanned aerial vehicles for high-resolution remote sensing to map invasive Phragmites australis in coastal wetlands. *International Journal of Remote Sensing*, 38(8–10), 2199–2217. https://doi.org/10.1080/01431161.2016.1239288
- Schieder, N. W., Walters, D. C., & Kirwan, M. L. (2018). Massive Upland to Wetland Conversion Compensated for Historical Marsh Loss in Chesapeake Bay, USA. *Estuaries and Coasts*, 41(4), 940–951. https://doi.org/10.1007/S12237-017-0336-9/FIGURES/6
- Silliman, B. R., & Bertness, M. D. (2004). Shoreline Development Drives Invasion of Phragmites australis and the Loss of Plant Diversity on New England Salt Marshes. *Conservation Biology*, 18(5), 1424–1434. https://doi.org/10.1111/J.1523-1739.2004.00112.X
- SMILE. (2022). RandomForest. Retrieved May 18, 2022, from http://haifengl.github.io/api/java/smile/regression/ RandomForest.html
- Smith, J. A. M. (2013). The Role of Phragmites australis in Mediating Inland Salt Marsh Migration in a Mid-Atlantic Estuary. PLoS ONE, 8(5), e65091. https://doi.org/10.1371/ JOURNAL.PONE.0065091
- Sweet, W.V, B.D. Hamlington, R.E. Kopp, C.P. Weaver, P.L. Barnard, D. Bekaert, W. B., M. Craghan, G. Dusek, T. Frederikse, G. Garner, A.S. Genz, J.P. Krasting, E. Larour, D. M., J.J. Marra, J. Obeysekera, M. Osler, M. Pendleton, D. Roman, L. Schmied, W. Veatch, K. D. W., & Zuzak, and C. (2022). Global and Regional Sea Level Rise Scenarios for the United States: Updated Mean Projections and Extreme Water Level Probabilities Along U.S. Coastlines. Retrieved from https://aambpublicoceanservice.blob.core.windows.net/oceanserviceprod/hazards/sealevelrise/noaa-nos-techrpt01-global-regional-SLR-scenarios-US.pdf
- Taylor, L., Curson, D., Verutes, G. M., & Wilsey, C. (2020). Mapping sea level rise impacts to identify climate change adaptation opportunities in the Chesapeake and Delaware Bays, USA. Wetlands Ecology and Management, 28(3), 527–541. https://doi.org/10.1007/S11273-020-09729-W/TABLES/2
- Townshend, J. R. G., Goff, T. E., & Tucker, C. J. (1985). Multitemporal Dimensionality of Images of Normalized Difference Vegetation Index at Continental Scales. *IEEE Transactions on Geoscience and Remote Sensing*, GE-23(6), 888–895. https://doi.org/10.1109/TGRS.1985.289474
- Tucker, C. J., Townshend, J. R. G., & Goff, T. E. (1985). African Land-Cover Classification Using Satellite Data. Science, 227(4685), 369–375. https://doi.org/10.1126/SCIENCE.227.4685.369
- Tulbure, M. G., & Johnston, C. A. (2010). Environmental conditions promoting non-native phragmites australis expansion in great lakes coastal wetlands. Wetlands, 30(3), 577–587. https://doi.org/10.1007/S13157-010-0054-6/TABLES/4
- Tully, K., Gedan, K., Epanchin-Niell, R., Strong, A., Bernhardt, E. S., Bendor, T., & Weston, N. B. (2019). The Invisible Flood: The Chemistry, Ecology, and Social Implications of



- Coastal Saltwater Intrusion. *BioScience*, 69(5), 368–378. https://doi.org/10.1093/BIOSCI/BIZ027
- U.S. Fish & Wildlife Service. (2018). National Wetlands Inventory. U.S. Fish & Wildlife Service. https://data.nal.usda.gov/dataset/national-wetlands-inventory. Accessed 18 May 2022.
- Vitousek, P. M., D'Antonio, C. M., Loope, L. L., & Westbrooks, R. (1996). Biological invasions as global environmental change. *American Scientist*, 84(5), 468–478.
- Walter, M., & Mondal, P. (2019). A Rapidly Assessed Wetland Stress Index (RAWSI) Using Landsat 8 and Sentinel-1 Radar Data. Remote Sensing, 11(21), 2549. https://doi.org/ 10.3390/rs11212549
- Wilcox, K. L., Petrie, S. A., Maynard, L. A., & Meyer, S. W. (2003). Historical Distribution and Abundance of Phragmites australis at Long Point, Lake Erie. *Ontario. Journal* of Great Lakes Research, 29(4), 664–680. https://doi.org/ 10.1016/S0380-1330(03)70469-9
- Windham, L., & Lathrop, R. G. (1999). Effects of Phragmites australis (common reed) invasion on aboveground biomass and soil properties in brackish tidal marsh of the mullica river. New Jersey. Estuaries, 22(4), 927–935. https://doi. org/10.2307/1353072

- Wu, C., Peng, D., Soudani, K., Siebicke, L., Gough, C. M., Arain, M. A., & Ge, Q. (2017). Land surface phenology derived from normalized difference vegetation index (NDVI) at global FLUXNET sites. Agricultural and Forest Meteorology, 233, 171–182. https://doi.org/10.1016/J. AGRFORMET.2016.11.193
- Xie, Y., Zhang, A., & Welsh, W. (2015). Mapping wetlands and phragmites using publically available remotely sensed images. *Photogrammetric Engineering and Remote Sens*ing, 81(1), 69–78. https://doi.org/10.14358/PERS.81.1.69

**Publisher's Note** Springer Nature remains neutral with regard to jurisdictional claims in published maps and institutional affiliations.

Springer Nature or its licensor (e.g. a society or other partner) holds exclusive rights to this article under a publishing agreement with the author(s) or other rightsholder(s); author self-archiving of the accepted manuscript version of this article is solely governed by the terms of such publishing agreement and applicable law.

